Improved Treatment of Cyclic β-Amino Acids and Successful Prediction of β-Peptide Secondary Structure Using a Modified Force Field: AMBER*C

LAURIE A. CHRISTIANSON, MELISSA J. LUCERO, DANIEL H. APPELLA, DANIEL A. KLEIN, SAMUEL H. GELLMAN

Department of Chemistry, University of Wisconsin, Madison, Wisconsin 53706

Received 18 August 1999; accepted 7 February 2000

ABSTRACT: We added parameters to the AMBER* force field to model cyclic β-amino acid derivatives more accurately within the commonly used MacroModel program. In an effort to generate an improved treatment of cyclohexane and cyclopentane conformational preferences, carbon–carbon torsional parameters were modified and incorporated into a force field we call AMBER*C. Simulation of *trans*-2-aminocyclohexanecarboxylic acid (*trans*-ACHC) and *trans*-2-aminocyclopentanecarboxylic acid (*trans*-ACPC) derivatives using AMBER*C produces more realistic energy differences between (pseudo)diaxial and (pseudo)diequatorial conformations than does simulation using AMBER*. AMBER*C molecular dynamics simulations more accurately reproduce the experimental hydrogen-bonding tendencies of simple diamide derivatives of *trans*-ACHC and *trans*-ACPC than do simulations using the AMBER* force field. More importantly, this modified force field allows accurate qualitative prediction of the helical secondary structures adopted by β-amino acid homo-oligomers.
 J Comput Chem 21: 763–773, 2000

Keywords: β-amino acids; β-peptides; force field; secondary structure; cycloalkane conformation

Correspondence to: S. H. Gellman; e-mail: gellman@chem.wisc.edu

Contract/grant sponsor: NIH; contract/grant number: GM56414

Introduction

The well-defined conformations assumed by proteins and nucleic acids are central to their roles in living organisms. Unnatural oligomers and polymers that also assume ordered, stable structures ("foldamers") could be used to create new chemical functions (e.g., catalysis) and to probe the factors that control conformational order in biopolymers.[1] Several types of foldamer backbones have recently been described.[2–22]

The origins of protein folding preferences have been studied for decades. While many of the underlying forces are partially understood, it is still challenging to design a conventional peptide of any size with complete control of the final three-dimensional structure.[23] The problem of molecular design becomes considerably more challenging with an unnatural backbone. We anticipated that it would be difficult to generate new periodic backbones that favor discrete, compact conformations if we searched empirically for such structures (i.e., by synthesizing and evaluating alternative oligomers). We therefore decided to explore the possibility that computer simulations could be used to identify monomers that would provide oligomers with specific folding propensities.

Experimental model studies from this laboratory have suggested that oligomers constructed from β-amino acids ("β-peptides") will avoid hydrogen bonds between nearest neighbor amide groups along the backbone.[24] β-Amino acids are therefore attractive building blocks for construction of foldamers, because avoidance of nearest-neighbor attractive interactions appears to be important for adoption of compact secondary structures.[24] We have recently shown that short β-peptides constructed from cycloalkane-based residues do indeed adopt stable helical conformations, and that modification of the cycloalkane backbone results in a change in helix shape.[3] β-Peptides built from acyclic residues can also form helices[2, 4, 5] or sheets.[6] Here, we describe the modification of an existing force field (AMBER*) for use in identifying β-amino acids (and other extended amino acids) that are promising candidates for foldamer construction. The resulting force field, AMBER*C, played a crucial role in the design of the helical[3] and sheet β-peptides[6a, 6b] we have reported.

Computational Methods

All studies were performed using MacroModel[25] 5.0. We used either the November 29, 1995, update to AMBER*[26] or our AMBER*C modified force field, as discussed below. All simulations made use of GB/SA chloroform continuum solvation model.[27] We chose AMBER* because this force field had the smallest number of low-quality bend, stretch, and torsion parameters for β-amino acid residues among the force fields available in MacroModel 5.0.

Torsional Monte Carlo (MC) conformational searches were performed as implemented in MacroModel.[28] During MC conformational searches, we generated 1000 starting structures, which were minimized to a gradient of 0.05 kJ/Å · mol, and structures within 6.0 kcal/mol (25 kJ/mol) of the lowest conformation were retained. Multiple simulations were performed from different starting conformations to verify that the same sets of conformations were found for each molecule.

Stochastic dynamics (SD)[29] and mixed Monte Carlo/stochastic dynamics (MC/SD)[30] simulations were performed as implemented in MacroModel. SD and MC/SD runs were all 1 ns in length using 0.5-fs time steps at 300 K. The bath constants were the default values, 0.2 ps for molecular dynamics and $\gamma = 1/2t$ for stochastic dynamics. There was no equilibration period. Dihedral angles and the presence of hydrogen bonds were monitored continuously during the run as described below. To establish that molecular behavior is not dependent on initial state for the oligomers, dynamics calculations were followed by several simulated annealing runs using different starting conformations.

Continuous cooling annealing protocols were similar for the *trans*-ACHC and *trans*-ACPC oligomers. The *trans*-ACHC decamer was equilibrated at 1000 K for 100 ps using a 1.5-fs timestep. Continuous cooling over 1000 ps was then initiated from 1000 K, ending at 50 K, using a 1.5-fs time step and 0.2-ps bath time constant. Constraints were added to the ring to prevent flipping into a diaxial orientation, as discussed below. The *trans*-ACPC oligomer was equilibrated at 600 K for 50 ps with a 1-fs timestep. Cooling from 600 to 50 K with a 1-fs timestep with a 0.2-ps bath constant took 400 ps. No constraints were used in the ACPC simulations.

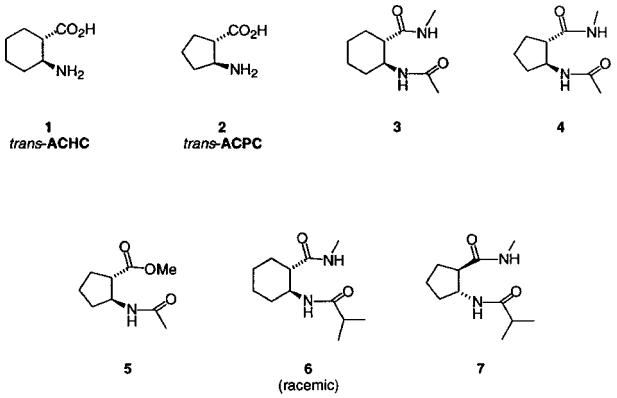

CHART 1.

Results and Discussion

AMBER* SIMULATIONS

Using AMBER* as is implemented in MacroModel, we examined the nearest-neighbor hydrogen-bonding capabilities (i.e., hydrogen bonding between adjacent amide groups) of β-peptides composed of *trans*-2-aminocyclohexanecarboxylic acid (*trans*-ACHC, **1**, Chart 1) and *trans*-2-aminocyclopentanecarboxylic acid (*trans*-ACPC, **2**, Chart 1), through the use of diamide derivatives **3** and **4** (Chart 1). We performed torsional Monte Carlo conformational searches for both **3** and **4**. In each case, the search located eight structures within 6 kcal/mol of the lowest minimum found.

For the diamide of *trans*-ACHC (**3**), the most stable conformer is a chair with both substituents axial. The second conformer is 2.5 kcal/mol higher in energy; both substituents are equatorial and form an eight-membered hydrogen-bonded ring. A third structure adopts a twist-boat conformation and is only 1.0 kcal/mol higher than the diequatorial structure. These results are contrary to expectation for this system. A values of similar substituents on cyclohexane[31] suggest that the diequatorial structure should be favored by at least 2.5 kcal/mol over the diaxial conformation. Intramolecular hydrogen bonding is computed to be stabilizing, as a diequatorial structure without hydrogen bonding is 2.1 kcal/mol higher in energy than the structure containing the eight-membered hydrogen-bonded ring.

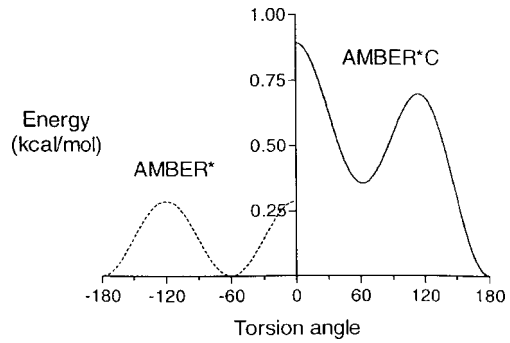

FIGURE 1. X—C—C—X torsional parameter in AMBER* and AMBER*C.

Eight-membered hydrogen-bonded rings dominate the conformations of the *trans*-ACPC diamide (**4**) in AMBER* simulations. The structure lowest in energy has the two substituents opposite the "flap" of an envelope conformation. The carbonyl on C_α eclipses the hydrogen on C_β, and the nitrogen on C_β eclipses the hydrogen on C_α (the N—C_β—C_α—C(=O) dihedral angle is 124°). Of the eight structures within 6.0 kcal/mol of the lowest structure found, seven have a N—C_β—C_α—C(=O) angle of 118° or greater, i.e., seven are eclipsed or pseudodiaxial structures. The only structure with pseudodiequatorial substituents (N—C_β—C_α—C(=O) dihedral angle of 95°) is 4.3 kcal/mol higher in energy than the lowest structure found.

Further examination of the computational results revealed that some of the preference of AMBER* for diaxial or pseudodiaxial conformations results from use of generic X—C—C—X torsional potentials. AMBER* uses the same threefold torsional expression ($E_{\text{tors}} = 0.144(1 + \cos[3\phi])$) to model all 24 torsions in the ring of **3** and all 20 torsions in the ring of **4**, regardless of whether the torsional interaction involves H—C—C—H, C—C—C—C or something else. In molecular mechanics force fields, nonbonded parameters (i.e., van der Waals, electrostatic) provide some of the energy of interactions between substituents on opposite ends of a bond. Torsional potentials modify the effects of nonbonded parameters, to provide the remainder of the 1,4-interaction energy, but the X—C—C—X torsional energy function in AMBER* does not position cycloalkane conformers accurately enough for our purposes.[32] Much of the "diaxial effect" in this particular system appears to be due to electrostatic repulsions between the amide groups, because differences among conformers of dialkylcyclohexanes are less pronounced than differences among conformers of **3** and **4** (see below).

TABLE I.
Comparison of Parameters for X—C—C—X Torsional Interactions: AMBER*[26] and AMBER*C.

$$E_{tors} = \frac{V_1}{2}(1 + \cos\phi) + \frac{V_2}{2}(1 - \cos[2\phi]) + \frac{V_3}{2}(1 + \cos[3\phi])$$

Force field	Parameter	Energy (kcal/mol) $V_1/2$	$V_2/2$	$V_3/2$
AMBER*	X—C—C—X (all)	0.000	0.000	0.144
AMBER*C	X—C—C—X	0.189	0.049	0.258
	X—C—C—H	0.000	0.000	0.144
	H—C—C—H	0.000	0.000	0.121

CREATION OF AMBER*C

To obtain energy differences among conformations of **3** and **4** that are in better accord with precedent, we altered the X—C—C—X parameters for all-atom AMBER* so that the force field's treatment of *n*-butane more closely resembled that of MM3*, which is considered to be an excellent model for alkanes.[33] (McDonald and Still performed an analogous procedure to adjust the energy differences between *gauche* and anti-conformations of alkyl chains for united-atom AMBER*.[34]) Additional H—C—C—H and H—C—C—X parameters were added to the X—C—C—X parameter (Table I). We reduced the H—C—C—H parameter by 16% to make the AMBER* treatment of ethane match that of MM3*. We then examined neopentane (which has only the H—C—C—C torsion) using both AMBER* and MM3*, and decided that the AMBER* H—C—C—X parameter (where X is any nonhydrogen atom) should be left unchanged. Finally, we incorporated these parameters into AMBER*. The modified force field was then used to evaluate the energy of rotation around the C—C—C—C torsion angle of *n*-butane to fit the remaining X—C—C—X parameter for the molecule. The threefold term $V_{3/2}(1 + \cos[3\phi])$, the barrier to eclipsing interactions, was raised, and onefold and twofold terms were added to make a *gauche* configuration torsionally more expensive than an anti-configuration of the carbon chain. Figure 1 compares the original and modified X—C—C—X parameters.

We term the force field with these new and modified torsional parameters AMBER*C (Table I), after McDonald and Still's AMBER*B united atom modifications.[34] A more elaborate treatment of the ACHC/ACPC ring system would evolve separate parameters for each combination of end groups in the system (H—C—C—N, C—C—C—C(=O), etc.). Unfortunately, we found it difficult to generate such a parameter set that was transferable to a range of cycloalkane-based β-amino acids under consideration, without elaborate use of special substructures for particular residues.[35] The current parameter set is sufficient to shift the relative energies among diequatorial, diaxial, eclipsed, and twist-boat conformers of substituted cycloalkyl β-amino acids so as to correspond to the available physical data, as discussed below. AMBER*C energy differences among *n*-butane conformations are virtually identical to those found under MM3*.[33]

EVALUATION OF AMBER*C

Geometry Optimizations

AMBER*C was tested by examining this force field's treatment of monoalkyl cyclohexanes. Although A values (ΔG°) have been determined for an enormous range of substituents on cyclohexane,[36] ΔH° differences between axial and equatorial substitution patterns, which correspond more closely to the steric energy differences found by molecular mechanics, are less well studied. Booth and Everett[37] and later Squillacote[38] have determined ΔH° (axial vs. equatorial) for methyl-, ethyl-, and isopropylcyclohexane. As shown in Table II, the calculated steric energy differences between ring conformers using AMBER*C correspond more closely to the experimental results than do the differences calculated by AMBER*.

When diamides **3** and **4** were modeled with the preliminary AMBER*C force field, we found that an AMBER* substructure for isopropylcarboxamide

TABLE II.
Experimental Conformational Enthalpy Values[40] and Calculated Steric Energy Differences between Axial and Equatorial Alkylcyclohexane Conformers (RC_6H_{11}).

R group	ΔH° (exp.)[a]	E_{steric} (calc.) AMBER*	AMBER*C
Me	-1.75 ± 0.05	-1.03	-1.75
Et	-1.60 ± 0.06	-1.10	-1.82
iPr	-1.52 ± 0.06	-1.10	-1.80

[a] $H^\circ_{(axial)} - H^\circ_{(equatorial)}$.

TABLE III.
Relative Steric Energy Differences for 3 and 4 from Monte Carlo Simulations[a] Using AMBER* and AMBER*C.

Compound	Conformation	E_{steric} (kcal/mol) AMBER*	AMBER*C
3 (*trans*-ACHC diamide)	diequatorial	0.00	0.0
	diaxial	−2.5	0.1
	twist-boat	1.0	2.8
4 (*trans*-ACPC diamide)	eclipsed	0.00	0.0
	pseudodiequatorial	4.3	1.7
	pseudodiaxial	4.7	2.1

[a] GB/SA $CHCl_3$.

was being matched against the *N*-methyl amide and adjacent ring carbons. It was not clear that the isopropylcarboxamide parameters were intended for this broad application,[39] and the charges assigned to the atoms by the parameters produced large electrostatic repulsions when we examined oligomers of *trans*-ACHC and *trans*-ACPC,[35] which led to inaccuracies in the modeling of these oligomers. These electrostatic interactions also contribute to the exaggerated preference for diaxial conformations of **3** and pseudodiaxial conformations of **4** by AMBER*, because diaxial conformations place the amide substituents further apart than do pseudodiequatorial conformations. Because the isopropylcarboxamide substructure was apparently intended for the end of a molecule rather than for repeated use throughout a molecule,[39] we narrowed the definition of the substructure by giving it explicit hydrogens, so that AMBER*C would not recognize the substructure for cycloalkylcarboxamides.

Torsional Monte Carlo Conformational Searches

Torsional Monte Carlo conformational searches for the diamides **3** and **4** were carried out using the AMBER*C force field. Table III summarizes the comparison between the AMBER* and AMBER*C results. For *trans*-ACHC diamide **3** using AMBER*C, 13 structures are within 6.0 kcal/mol of the lowest minimum found, which is a hydrogen-bonded diequatorial structure (Fig. 2a). This conformation, another with equatorial amides (not shown), and one with axial amides (Fig. 2b) are less than 0.1 kcal/mol apart in steric energy. This result conflicts with the ca. 2.5 kcal/mol preference for diequatorial relative to diaxial conformations expected for this molecule on the basis of A values;[31,36] nevertheless, the AMBER*C result represents an improvement compared to original AMBER* in that the favored structure now has diequatorial substituents. Figure 2c illustrates a diequatorial conformation without hydrogen bond-

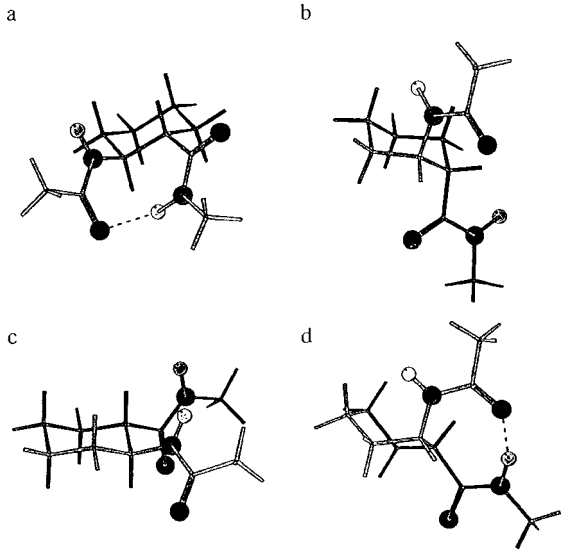

FIGURE 2. Representative conformations of *trans*-ACHC derivative **3** from an AMBER*C Monte Carlo conformational search. All figures of computational structures were produced with Molscript (Kraulis, P. J. Appl Crystallogr 1991, 24, 946). Oxygen is shown in black, nitrogen in gray, and amide hydrogens in white. Hydrogen bonds are shown as dashed lines. (a) Diequatorial conformation with an eight-membered hydrogen-bonded ring (relative energy, 0 kcal/mol). (b) Diaxial conformation (relative energy, +0.1 kcal/mol). (c) Diequatorial conformation without hydrogen bonding (relative energy, +1.4 kcal/mol). (d) Twist-boat conformation with an eight-membered hydrogen-bonded ring (relative energy, +2.8 kcal/mol).

ing. Twist-boat structures of **3** are less prominent with AMBER*C than with AMBER*, which also seems to reflect an improvement. The lowest energy twist-boat structure (Fig. 2d) is 2.8 kcal/mol above the most stable conformation, and higher in energy than both chair conformations.

Of the eight structures found for **3** in the AMBER*C torsional MC conformational search, six have corresponding structures in the AMBER* torsional MC conformational search. All such pairs of structures are identical to within 0.135 Å r.m.s. difference between heavy atoms. Thus, it appears that the reparameterization has altered the steric energy differences among the structures located by the conformational search, but that there is little, if any, effect on the conformations themselves.

The AMBER*C torsional Monte Carlo conformational search of *trans*-ACPC diamide **4** located 12 structures within 6 kcal/mol of the lowest minimum. The family of structures is dominated by the formation of eight-membered hydrogen bonded rings, as was seen in the simulation using AMBER*, and the lowest minimum is a C_α—C_β eclipsed conformation that is identical to the lowest energy structure found with AMBER* to within 0.178 Å r.m.s. for the heavy atoms (Fig. 3a).

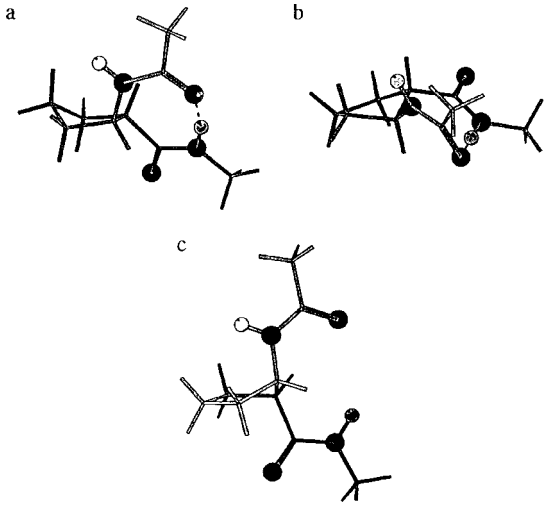

FIGURE 3. Representative conformations of *trans*-ACPC derivative **4** from AMBER*C Monte Carlo simulation. Oxygen is shown in black, nitrogen in gray, and amide hydrogens in white. Hydrogen bonds are shown as dashed lines. (a) Eclipsed conformation with an eight-membered hydrogen-bonded ring (relative energy, 0 kcal/mol). (b) Pseudodiequatorial conformation with an eight-membered hydrogen-bonded ring (relative energy, +1.7 kcal/mol). (c) Pseudodiaxial conformation (relative energy, +2.1 kcal/mol).

However, the third most stable structure found with AMBER*C has an eight-membered hydrogen-bonded ring and pseudoequatorial substituents (Fig. 3b), 1.7 kcal/mol above the minimum. This pseudodiequatorial structure has a N—C_β—C_α—C(=O) dihedral angle of 71°, similar to the crystal structures of *trans*-ACPC derivatives (ref. 40, and unpublished results), but is unlike any structures identified by AMBER*. Figure 3c shows a pseudodiaxial conformation with a N—C_β—C_α—C(=O) dihedral angle of 163°.

Only three of the eight AMBER* conformers of **4** correspond to the AMBER*C structures, and several of the remaining conformers have no low energy AMBER*C analogs at all. The two force fields produce conformational families that differ significantly because the cyclopentyl ring torsions do not lie at minima for the X—C—C—X energy profile. Thus, unlike the simulations of *trans*-ACHC derivative **3**, simulations of **4** exhibit different preferred ring conformations for each version of the force field. In particular, AMBER*C predicts pseudodiequatorial conformations of *trans*-ACPC derivatives that are flatter through the N—C_β—C_α—C(=O) dihedral angle than are conformations predicted by AMBER*. Conformations such as that shown in Figure 3b appear to reproduce more accurately the conformational preferences of *trans*-ACPC as seen in crystal structures of several derivatives (ref. 40, and unpublished results) than do the AMBER*-predicted conformations.

Molecular and Stochastic Dynamics Simulations

We used molecular dynamics to examine the amount of time **3** and **4** spent in various conformations. In particular, we wanted to evaluate the relative amount of intramolecular hydrogen bonding each molecule experienced. The relative extent of hydrogen bonding in **3** and **4** could also be evaluated experimentally, and compared with the results of our simulations, to gauge the reliability of these simulations.

We were unable to examine a fully equilibrated system containing both diequatorial and diaxial conformers of **3**, because interconversion of these conformers is slow. In fact, we would have been surprised to observe such an interconversion, because the barrier between the two chair forms of cyclohexane is estimated to be 10–11 kcal/mol at 300 K.[41] In our 1-ns simulations, no interconversions occurred starting from either the diequatorial or diaxial state.[42] We, therefore, examined the extent

of hydrogen bonding in the diequatorial conformer over a 1-ns MC/SD simulation. (We anticipate that the diequatorial conformation should be the dominant conformation in solution.) An eight-membered hydrogen-bonded ring was present to a similar extent under both force fields: 27% of the time with AMBER*, 25% with AMBER*C. A six-membered hydrogen-bonded ring was completely disallowed using AMBER*, but was present 1% of the time using AMBER*C.

The stochastic dynamics simulations of *trans*-ACPC diamide **4** explored pseudodiaxial as well as pseudodiequatorial structures because of the compound's greater conformational flexibility relative to **3**. Stochastic dynamics simulations (not mixed mode) were, therefore, sufficient to evaluate the equilibrated system. In a 1-ns SD simulation under AMBER*, an eight-membered hydrogen-bonded ring was present 28% of the time, while under AMBER*C this hydrogen-bonded ring was present 66% of the time.

The eclipsing conformation of **4** dominated the distribution of structures for both AMBER* and AMBER*C. Figure 4 shows the distribution of the N—C_β—C_α—C(=O) dihedral angle during the two stochastic dynamics simulations. Using either force field, the predominant dihedral angle values range from 110 to 130°, corresponding to the eclipsed "back of the envelope" arrangement of the substituents (Figs. 2a and 3a). This structure dominated the AMBER*C simulation, as reflected in its high hydrogen-bonded percentage relative to the AMBER* simulation. The distribution for the AMBER* simulation shows a large spike at 150 to 160°, in addition to the spike at 120 to 130°, reflecting the strong pseudodiaxial preference for **4**. This tendency contributes to the smaller hydrogen-bonded percentage observed using AMBER*. This

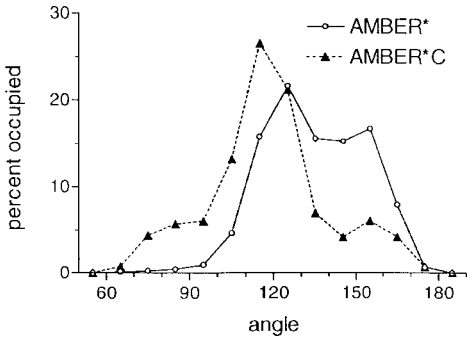

FIGURE 4. Distribution of N—C_β—C_α—C(=O) dihedral angle during SD simulations of **4**.

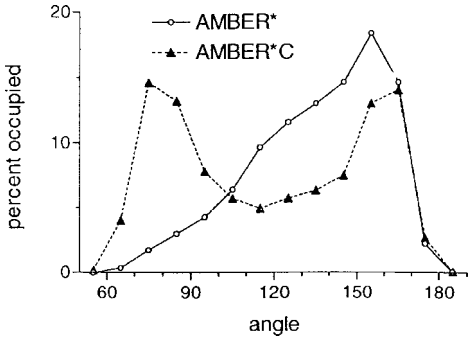

FIGURE 5. Distribution of N—C_β—C_α—C(=O) dihedral angle during SD simulations of **5**.

preference for the pseudodiaxial conformation is not observed in AMBER*C simulations.

To examine conformational preferences in the absence of hydrogen bonding, we conducted dynamics simulations of the acetamido-*trans*-ACPC methyl ester **5** (Chart 1), which cannot form an eight-membered hydrogen-bonded ring. Figure 5 shows the distribution of the N—C_β—C_α—C(=O) dihedral angle during the 1-ns SD runs on **5**. Lacking the dominating hydrogen bond of compound **4**, monoester **5** is observed mainly in a pseudodiaxial conformation using AMBER* (i.e., the N—C_β—C_α—C(=O) dihedral angle is about 160°), while with AMBER*C the molecule spends roughly equal amounts of time in pseudodiaxial and pseudodiequatorial (N—C_β—C_α—C(=O) ~80°) conformations. The eclipsed conformation found preferentially for diamide **4** occupies a cusp between the two well-populated conformers for monoester **5**, which cannot stabilize this eclipsed conformation with a hydrogen bond.

COMPARISON WITH EXPERIMENTAL DATA

AMBER* dynamics simulations indicated that **3** and **4** should experience intramolecular hydrogen bonding to an equal extent, while the AMBER*C studies predicted that **4** should experience much more internal hydrogen bonding than **3**. We examined these predictions experimentally by preparing related diamides **6** and **7** (Chart 1), which have isopropyl groups to enhance solubility in CH_2Cl_2. (Based on precedents involving conventional peptides, we did not expect the switch from methyl groups in **3** and **4** to isopropyl groups in **6** and **7** to exert a significant effect on internal hydrogen bonding.)

Diamides **6** and **7** were studied by IR spectroscopy at ca. 1 mM in CH_2Cl_2.[24] (Spectra taken at

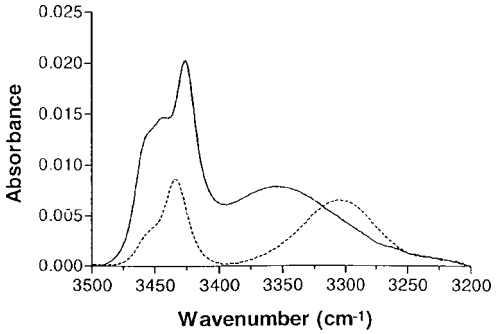

FIGURE 6. N—H stretching region of IR spectra for compounds **6** (solid line) and **7** (dotted line). Spectra obtained at ca. 1 mM in CH_2Cl_2.

several concentrations indicated that neither molecule aggregated at 1 mM.) The N—H stretch region of each IR spectrum is presented in Figure 6. Qualitative comparison indicates that *trans*-ACPC derivative **7** experiences more intramolecular hydrogen bonding than does *trans*-ACHC derivative **6** (compare relative intensities of hydrogen bonded absorbances ($<3400\ cm^{-1}$) and nonhydrogen bonded absorbances ($>3400\ cm^{-1}$)), in accordance with the AMBER*C prediction, but contrary to the AMBER* prediction. It is also noteworthy that the hydrogen bonded peak for **6** is at $3357\ cm^{-1}$, while the hydrogen bonded peak for **7** is at $3306\ cm^{-1}$, suggesting that the C=O and H—N in **6** are not oriented as favorably for a strong hydrogen bond as are the corresponding C=O and H—N in **7**. Amide–amide hydrogen bond energy is optimal when the N—H···O angle is 180°.[43] In the hydrogen bonded conformations of cyclohexane-based **3** resulting from MC conformational searches, the hydrogen bond N—H···O angle deviates significantly from linearity (e.g., the conformation shown in Fig. 2a, with an N—H···O angle of 151°). On the other hand, in the conformations of cyclopentane-based **4** obtained from MC conformational searches, the N—H···O angle in the eight-membered hydrogen bonded ring is closer to linear (e.g., the conformations shown in Fig. 3a and b, with N—H···O angles of 164 and 167°, respectively).

EXTENSION TO β-AMINO ACID OLIGOMERS

While the results with monomers **3** and **4** were promising, our intent in creating AMBER*C was to ensure that we could use a standard force field to model oligomers of β-amino acids. We, therefore, tested our modified force field by modeling β-peptides composed of *trans*-ACHC or *trans*-ACPC residues and comparing the simulated conformations with X-ray structures. Preliminary AMBER* simulations suggested that *trans*-ACHC oligomers would adopt a helical conformation specified by 14-membered ring hydrogen bonds that occur between each carbonyl oxygen and the amide proton of the second residue toward the N-terminus (Fig. 7). Oligomers of *trans*-ACPC were predicted to favor a very different helix, specified by 12-membered ring hydrogen bonds that occur between each carbonyl oxygen and the amide proton of the third residue toward the C-terminus.[35] We tested these predictions with more rigorous simulations involving AMBER*C.

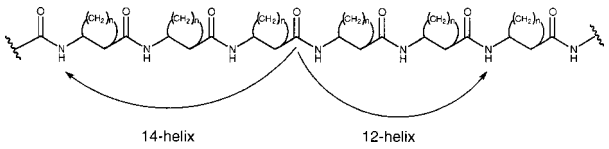

FIGURE 7. Characteristic backbone hydrogen bonds associated with the β-peptide 14-helix, and 12-helix.

trans-ACHC Oligomers

We conducted a MC/SD simulation of Ac(*trans*-ACHC)$_{10}$NHMe, followed by multiple, rigorous simulated annealing runs.[44] Using GB/SA continuum chloroform solvation, the decamer was equilibrated at 1000 K for 100 ps with 1.5-fs time steps, starting in a 12-helix, and allowed to cool to 50 K over 1000 ps using 1.5-fs time steps. Constraints were added to prevent the rings from flipping into a diaxial orientation (a flat-bottomed, onefold torsional barrier with a force constant of 1000 kJ/mol, N—C_β—C_α—C(=O) dihedral angles constrained to 55 ± 10°). This annealing procedure was repeated three times, each time utilizing different initial atomic velocities. All three simulations cooled to a 14-helical conformation. The r.m.s. difference in the positions of the heavy atoms was no more than 0.010 Å, suggesting that when only diequatorial rings are allowed, the 14-helix is the most stable conformation available to the *trans*-ACHC decamer.

Experimentally, tBoc(*trans*-ACHC)$_4$OBn and tBoc(*trans*-ACHC)$_6$OBn both assume the 14-helix in the solid state,[3a,3e] and tBoc(*trans*-ACHC)$_4$OBn displays the 14-helical conformation in methanol[3g] (the hexamer was difficult to analyze by NMR because of resonance overlap). Solubility problems preclude the synthesis of longer ACHC oligomers. More recent work has shown that β-peptide hexamers containing *trans*-ACHC and other residues adopt the 14-helix in aqueous solution.[3d]

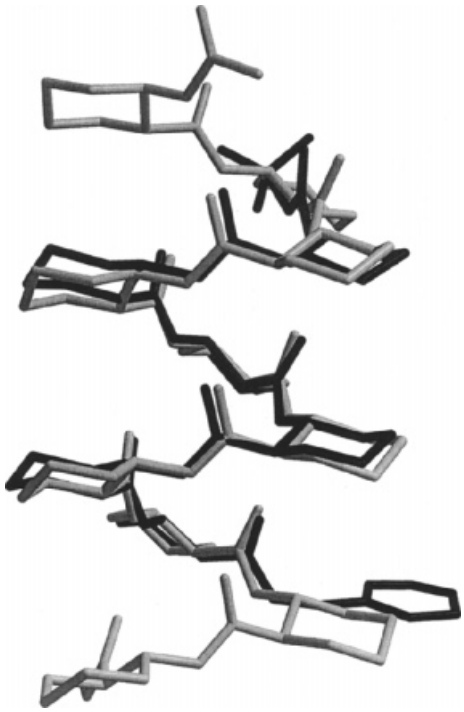

FIGURE 8. Crystal structure of tBoc(*trans*-ACHC)$_6$OBn overlaid on the calculated low-energy 14-helical conformation of Ac(*trans*-ACPC)$_{10}$NHMe. The crystal structure is in black, and the calculated structure is in gray; the calculated structure was obtained from simulated annealing starting from a 12-helical conformation, with the cyclohexyl rings constrained to remain diequatorial (see text).

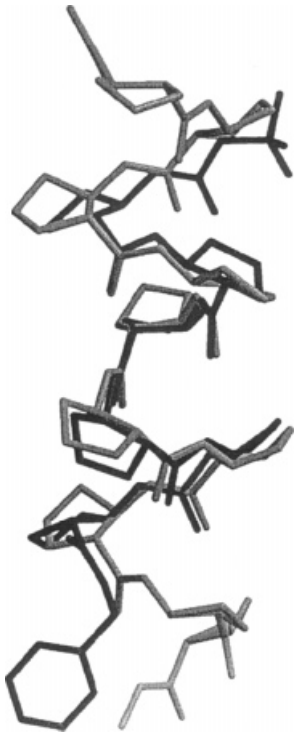

FIGURE 9. Crystal structure of tBoc(*trans*-ACPC)$_8$OBn overlaid on the calculated low-energy 12-helical conformation of Ac(*trans*-ACPC)$_{10}$NHMe. The crystal structure is in black, and the calculated structure is in gray. The calculated structure was obtained from simulated annealing (see Fig. 11a and the text).

The crystal structures of tBoc(*trans*-ACHC)$_4$OBn and tBoc(*trans*-ACHC)$_6$OBn may be overlaid on the computationally predicted 14-helical conformation of the decamer, aligning both the cyclohexyl rings and the backbone, as illustrated in Figure 8.

trans-ACPC OLIGOMERS

MC/SD simulations and simulated annealing studies conducted for Ac(*trans*-ACPC)$_{10}$NHMe indicate a strong preference for the 12-helix. The annealing procedure began with 50 ps of equilibration at 600 K, with 1-fs time steps, following by cooling to 50 K over 400 ps, again with 1-fs time steps. Six simulations starting from 12-helical, 14-helical, or random conformations were run, with all but one reverting to a perfect 12-helical conformation. The largest r.m.s. difference in the location of the heavy atoms among the five 12-helical conformations was 0.079 Å. The slightly less stable outlier forms a 12-helix for the first eight residues and then opens into 16-membered hydrogen bonded rings.

The AMBER*C predictions were tested experimentally through the synthesis and characterization of two *trans*-ACPC oligomers: tBoc(*trans*-ACPC)$_6$OBn and tBoc(*trans*-ACPC)$_8$OBn. Both molecules assume 12-helical conformations in the solid state and in pyridine-d$_6$.[3b, 3f, 3g] We have recently shown that β-peptides containing *trans*-ACPC and related residues display the 12-helical conformation in aqueous solution.[3h] The simulated 12-helix overlays well on the crystal structure, as can be seen in Figure 9. Although there is some variation in the local conformation of the cyclopentyl rings, there is excellent overlap along the backbones.

Conclusion

Our modest reparameterization of AMBER* provides a somewhat improved treatment of cyclic β-amino acids: diaxial and twist-boat conformations of *trans*-ACHC derivatives are displaced to higher energies relative to diequatorial conformations, and *trans*-ACPC derivatives are more accurately modeled. Using a combination of MC/SD simulations

and simulated annealing with AMBER*C, we were able to generate qualitatively accurate predictions of novel helical conformations adopted by homo-oligomers of *trans*-ACHC or *trans*-ACPC in the solid state, and by oligomers containing these residues in a variety of solvents.

Acknowledgments

We thank M. Richards for technical assistance.

References

1. Recent reviews: (a) Gellman, S. H. Acc Chem Res 1998, 31, 173; (b) Kirshenbaum, K.; Zuckermann, R. N.; Dill, K. A. Curr Opin Struct Biol 1999, 9, 530.
2. (a) Seebach, D.; Overhand, M.; Kühnle, F. N. M.; Martinoni, B.; Oberer, L.; Hommel, U.; Widmer, H. Helv Chim Acta 1996, 79, 913; (b) Seebach, D.; Ciceri, P.; Overhand, M.; Juan, B.; Rigo, D.; Oberer, L.; Hommel, U.; Amstutz, R.; Widmer, H. Helv Chim Acta 1996, 79, 2043; (c) Seebach, D.; Matthews, J. L. J Chem Soc Chem Commun 1997, 2015; (d) Seebach, D.; Abele, S.; Gademann, K.; Guichard, G.; Hintermann, T.; Juan, B.; Matthews, J. L.; Schreiber, J.; Oberer, L.; Hommel, U.; Widmer, H. Helv Chim Acta 1998, 81, 932; (e) Seebach, D.; Abele, S.; Sifferlen, T.; Hänggi, M.; Gruner, S.; Seiler, P. Helv Chim Acta 1998, 81, 2218.
3. (a) Appella, D. H.; Christianson, L. A.; Karle, I. L.; Powell, D. R.; Gellman, S. H. J Am Chem Soc 1996, 118, 13071; (b) Appella, D. H.; Christianson, L. A.; Klein, D. A.; Powell, D. R.; Huang, X.; Barchi, J. J.; Gellman, S. H. Nature 1997, 387, 381; (c) Applequist, J.; Bode, K. A.; Appella, D. H.; Christianson, L. A.; Gellman, S. H. J Am Chem Soc 1998, 120, 4891; (d) Appella, D. H.; Barchi, J. J.; Durell, S.; Gellman, S. H. J Am Chem Soc 1999, 121, 2309; (e) Appella, D. H.; Christianson, L. A.; Karle, I. L.; Powell, D. R.; Gellman, S. H. J Am Chem Soc 1999, 121, 6206; (f) Appella, D. H.; Christianson, L. A.; Klein, D. A.; Richards, M. R.; Powell, D. R.; Gellman, S. H. J Am Chem Soc 1999, 121, 7574; (g) Barchi, J. J.; Huang, X.; Appella, D. H.; Christianson, L. A.; Durell, S. R.; Gellman, S. H. J Am Chem Soc, to appear; (h) Wang, X.; Espinosa, J. F.; Gellman, S. H. J Am Chem Soc, to appear.
4. Gung, B. W.; Zou, D.; Stalcup, A. M.; Cottrell, C. E. J Org Chem 1999, 64, 2176.
5. Computer simulations of β-peptides: (a) Daura, X.; van Gunsteren, W. F.; Rigo, D.; Jaun, B.; Seebach, D. Chem Eur J 1997, 3, 1410; (b) Christianson, L. A. Ph.D. Thesis, University of Wisconsin–Madison (1997); (c) Daura, X.; Jaun, B.; Seebach, D.; van Gunsteren, W. F.; Mark, A. J Mol Biol 1998, 280, 925; (d) Daura, X.; Gademann, K.; Jaun, B.; Seebach, D.; van Gunsteren, W. F.; Mark, A. E. Angew Chem Int Ed Engl 1999, 38, 236; (e) Daura, X.; van Gunsteren, W. F.; Mark, A. E. Proteins Struct Funct Genet 1999, 34, 269; (f) Wu, Y. D.; Wang, D. P. J Am Chem Soc 1998, 120, 13485; (g) Möhle, K.; Günther, R.; Thormann, N.; Hofmann, H.-J. Biopolymers 1999, 50, 167.
6. (a) Krauthäuser, S.; Christianson, L. A.; Powell, D. R.; Gellman, S. H. J Am Chem Soc 1997, 119, 11719; (b) Chung, Y. J.; Christianson, L. A.; Stanger, H. E.; Powell, D. R.; Gellman, S. H. J Am Chem Soc 1998, 120, 10555; (c) Seebach, D.; Abele, S.; Gademann, K.; Jaun, B. Angew Chem Int Ed Engl 1999, 38, 1595.
7. Diederichsen, U.; Schmitt, H. W. J Org Chem 1998, 827.
8. Hagihara, M.; Anthony, N. J.; Stout, T. J.; Clardy, J.; Schreiber, S. L. J Am Chem Soc 1992, 114, 6568.
9. Beier, M.; Reck, F.; Wagner, T.; Krishnamurthy, R.; Eschenmoser, A. Science 1999, 283, 699, and references therein.
10. (a) Lokey, R. S.; Iverson, B. L. Nature 1995, 375, 303; (b) Nguyen, J. Q.; Iverson, B. L. J Am Chem Soc 1999, 121, 2639.
11. Gennari, C.; Salom, B.; Potenza, D.; Longari, C.; Fioravanzo, E.; Carugo, O.; Sardone, N. Chem Eur J 1996, 2, 644, and references therein.
12. (a) Hintermann, T.; Gademann, K.; Jaun, B.; Seebach, D. Helv Chim Acta 1998, 81, 983; (b) Hanessian, S.; Luo, X.; Schaum, R.; Michnick, S. J. J Am Chem Soc 1998, 120, 8569; (c) Hanessian, S.; Luo, X.; Schaum, R. Tetrahedron Lett 1999, 40, 4925.
13. Szabo, L.; Smith, B. L.; McReynolds, K. D.; Parrill, A. L.; Morris, E. R.; Gervay, J. J Org Chem 1998, 63, 1074.
14. (a) Smith, M. D.; Claridge, T. D. W.; Tranter, G. E.; Sansom, M. S. P.; Fleet, G. W. J. J Chem Soc Chem Commun 1998, 2041; (b) Long, D. D.; Hungerford, N. L.; Smith, M. D.; Brittain, D. E. A.; Marquess, D. G.; Claridge, T. D. W.; Fleet, G. W. J. Tetrahedron Lett 1999, 40, 2195; (c) Claridge, T. D. W.; Long, D. D.; Hungerford, N. L.; Aplin, R. T.; Smith, M. D.; Marquess, D. G.; Fleet, G. W. J. Tetrahedron Lett 1999, 40, 2199.
15. Nowick, J. S.; Mahrus, S.; Smith, E. M.; Ziller, J. W. J Am Chem Soc 1996, 118, 1066.
16. Hamuro, Y.; Geib, S. J.; Hamilton, A. D. J Am Chem Soc 1997, 119, 10587, and references therein.
17. (a) Armand, P.; Kirshenbaum, K.; Goldsmith, R. A.; Farr–Jones, S.; Barron, A. E.; Truong, K. T.; Dill, K. A.; Mierke, D. F.; Cohen, F. E.; Zuckermann, R. N.; Bradley, E. K. Proc Natl Acad Sci USA 1998, 95, 4309; (b) Kirshenbaum, K.; Barron, A. E.; Goldsmith, R. A.; Armand, P.; Bradley, E. K.; Truong, K. T.; Dill, K. A.; Cohen, F. E.; Zuckermann, R. N. Proc Natl Acad Sci USA 1998, 95, 4303.
18. (a) Nelson, J. C.; Saven, J. G.; Moore, J. S.; Wolynes, P. G. Science 1997, 277, 1793; (b) Prince, R. B.; Okada, T.; Moore, J. S. Angew Chem Int Ed Engl 1999, 38, 233; (c) Gin, M. S.; Yokozawa, T.; Prince, R. B.; Moore, J. S. J Am Chem Soc 1999, 121, 2643.
19. Yang, D.; Qu, J.; Li, B.; Ng, F.; Wang, X.; Cheung, K.; Wang, D.; Wu, Y. J Am Chem Soc 1999, 121, 589, and references therein.
20. Tanatani, A.; Yamaguchi, K.; Azumaya, I.; Fukutomi, R.; Shudo, K.; Kagechika, H. J Am Chem Soc 1998, 120, 6433, and references therein.
21. Smith, A. B.; Guzman, M. C.; Sprengler, P. A.; Keenan, T. P.; Holcomb, R. C.; Wood, J. L.; Carroll, P. J.; Hirschmann, R. J Am Chem Soc 1994, 116, 9947.
22. (a) Bassani, D. M.; Lehn, J.-M.; Baum, G.; Fenske, D. Angew Chem Int Ed Engl 1997, 36, 1845; (b) Bassani, D. M.; Lehn, J.-M. Bull Soc Chim Fr 1997, 134, 897.
23. (a) Betz, S. F.; Raleigh, D. P.; DeGrado, W. F. Curr Opin Struct Biol 1993, 3, 601; (b) Dahiyat, B. I.; Mayo, S. L. Science 1997, 278, 82.
24. Dado, G. P.; Gellman, S. H. J Am Chem Soc 1994, 116, 1054.

25. Mohamadi, F.; Richards, N. G. J.; Guida, W. C.; Liskamp, R.; Lipton, M.; Caufield, C.; Chang, G.; Hendrickson, T.; Still, W. C. J Comput Chem 1990, 11, 440.
26. (a) All-atom AMBER: Weiner, S. J.; Kollman, P. A.; Nguyen, D. T.; Case, D. A. J Comput Chem 1986, 7, 130; (b) AMBER* amide parameters: McDonald, D. Q.; Still, W. C. Tetrahedron Lett 1992, 33, 7743.
27. Still, W. C.; Tempczyk, A.; Hawley, R. C.; Hendrickson, T. J Am Chem Soc 1990, 112, 6127.
28. Chang, G.; Guida, W. C.; Still, W. C. J Am Chem Soc 1989, 111, 4379.
29. van Gunsteren, W. F.; Berendsen, H. J. C. Molec Simul 1988, 1, 173.
30. Guarnieri, F.; Still, W. C. J Comput Chem 1994, 15, 1302.
31. Eliel, E. L.; Wilen, S. H.; Mander, L. N. Stereochemistry of Organic Compounds; John Wiley & Sons, Inc: New York, 1994, p. 696.
32. Gundertofte, K.; Liljefors, T.; Norrby, P.-O.; Petterson, I. J Comput Chem 1996, 17, 429.
33. Allinger, N. L.; Yuh, Y. H.; Lii, J.-H. J Am Chem Soc 1989, 111, 8551.
34. McDonald, D. Q.; Still, W. C. J Am Chem Soc 1994, 116, 11550.
35. Christianson, L. A. Ph. D. Thesis, University of Wisconsin, Madison (1997).
36. Hirch, J. A. Top Stereochem 1967, 1, 199.
37. Booth, H.; Everett, J. R. J Chem Soc Perkin II 1980, 255.
38. Squillacote, M. E. J Chem Soc Chem Commun 1986, 1406.
39. Parish, C. A.; Still, W. C. Abstr Pap Am Chem Soc 1995, 210, 154-COMP.
40. Yamazaki, T.; Zhu, Y.-F.; Probstl, A.; Chadha, R. K.; Goodman, M. J Org Chem 1991, 56, 6644.
41. Eliel, E. L.; Wilen, S. H.; Mander, L. N. Stereochemistry of Organic Compounds; John Wiley & Sons, Inc: New York, 1994, p. 688.
42. We were unable to perform a simulation that adequately sampled all conformations using various mixed Monte Carlo/stochastic dynamics methods (ref. 30). Our attempted "Jumping Between Wells" (JBW) searches (Senderowitz, H.; Guarnieri, F.; Still, W. C. J Am Chem Soc 1995, 117, 8211) failed because we were unable to assemble a good set of torsion angles for interconversion of diaxial and diequatorial conformations (ref. 36).
43. Baker, E. N.; Hubbard, R. E. Prog Biophys Molec Biol 1984, 44, 97.
44. Early simulated annealing simulations indicated that nonfacile interconversion of ring conformations was a contributing factor to our inability to differentiate between helices. Individual residues were observed to interconvert among diaxial, twist-boat, and diequatorial conformations at the beginning of a cooling phase, but rapidly became trapped in one conformation before reaching room temperature.